ELSEVIER

Biophysical Chemistry 67 (1997) 151–158

Biophysical Chemistry

Multiple nucleosome positioning with unique rotational phasing on multimers of the light-responsive elements of pea *rbcS-3A* and *rbcS-3.6* genes: comparison between experimental and theoretical mapping

Rosalia Alessi [a], Stefano Cacchione [a,1], Pasquale De Santis [b], Mario Fuà [a,b], Maria Savino [a,*]

[a] *Istituto Pasteur–Fondazione Cenci Bolognetti, Dipartimento di Genetica e Biologia Moleculare, Università degli Studi di Roma 'La Sapienza', P.le A. Moro 5, 00185 Roma, Italy*

[b] *Dipartimento di Chimica, Università degli Studi di Roma 'La Sapienza', P.le A. Moro 5, 00185 Roma, Italy*

Received 21 October 1996; revised 21 January 1997; accepted 3 March 1997

Abstract

Nucleosome positioning along two DNA tracts, corresponding to tetramers of the light-responsive elements of pea *rbcS-3A* and *rbcS-3.6* genes, were studied by experimental (exonuclease III mapping and band shift electrophoresis) as well as theoretical methods.

Multiple nucleosome positioning with unique rotational phase was derived from both methods in satisfactorily good agreement, if nucleosome dyad axis positions are considered. Theoretical and experimental distributions of nucleosome frequencies appear different, probably on account of DNA sequence dependent digestion kinetics of exonuclease III. © 1997 Elsevier Science B.V.

Keywords: Nucleosome positioning; *rbcS* Light-responsive elements; LRE multimers; Theoretical methods for nucleosome positioning

1. Introduction

The role of DNA in nucleosome organization is mainly attributed to DNA anisotropic bendability, which determines the orientation of the DNA double helix with respect to the surface of the histone octamer [1]. DNA bendability is dictated by DNA sequence through the combination of local signals, mainly the roll angles of the 16 possible dinucleotides, according to a simple and successful nearest-neighbour approximation [2,3].

In the last few years, the attention of researchers has been focused on the relationships between DNA curvature and nucleosome positioning. In many cases curved sequences form nucleosomes more strongly than straight sequences, because less energy is required to bend them around histone octamers. Moreover, phased curved tracts give rise to multiple nu-

* Corresponding author. Tel: (39)-6-49912238; fax: (39)-6-4440812.

[1] E-mail address: s.cacchione@caspur.it

PII S0301-4622(97)00035-5

cleosome positioning with unique rotational phase. In nucleosomes, 146 base pairs of DNA are wrapped around the histone octamer; therefore, multiple positions differing by one helical repeat should be quasi-isoenergetic. However, multiple nucleosome positioning, far from being considered a rather obvious consequence of the Boltzmann distribution, could represent an important device for biological systems to regulate nucleosome dynamics [4–6] and the possibility for DNA sequences complexed with histone octamer to become readable for transcription factors.

Multimers of curved DNA tracts, in phase with B-DNA double helix, should assemble in nucleosomes having a unique rotational phase; therefore, they can be helpfully used to study multiple nucleosome positioning. Moreover, a number of virtual nucleosome positions spanning the same sequence, therefore characterized by equal curvature and chemical interactions, can be identified on DNA multimers. These features should be of help in testing the accuracy of experimental methods of nucleosome mapping.

Using the theoretical method developed in our research group [2,3], as well as experimental methods such as band shift assay and Exo III footprinting analysis, we have studied nucleosome organization on multimers of the light-responsive elements $(LRE)_4$ of two pea *rbcS* genes (see Fig. 1) [7]. The two LREs and their in-phase multimers have defined superstructural features [8] that influence their interactions with the polycation spermine [9], and should give rise to a well defined multiple nucleosome positioning.

$(LRE\text{-}3A)_4$

*Eco*RI *Sma*I
AATTCGAGCTCGGTACCC
ACACAAAATTTCAAATCTTGTGTGGTTAATATGGCTGCAAACTTTATCATTTTCACTATCTA
ACACAAAATTTCAAATCTTGTGTGGTTAATATGGCTGCAAACTTTATCATTTTCACTATCTA
ACACAAAATTTCAAATCTTGTGTGGTTAATATGGCTGCAAACTTTATCATTTTCACTATCTA
ACACAAAATTTCAAATCTTGTGTGGTTAATATGGCTGCAAACTTTATCATTTTCACTATCTA
ACACGGGGATCCTCTAGAGTCGACCTGCAGGCATGCA
*Sma*I *Hin*dIII

$(LRE\text{-}3.6)_4$

*Hin*dIII *Sma*I
TGCATGCCTGCAGGTCGACTCTAGAGGATCCCC
ACACACAACTTTTCAATCTTGTGTGGTTAATATGGCTGCAAAGTTTATCATTTCACAATCTA
ACACACAACTTTTCAATCTTGTGTGGTTAATATGGCTGCAAAGTTTATCATTTCACAATCTA
ACACACAACTTTTCAATCTTGTGTGGTTAATATGGCTGCAAAGTTTATCATTTCACAATCTA
ACACACAACTTTTCAATCTTGTGTGGTTAATATGGCTGCAAAGTTTATCATTTCACAATCTA
ACACGGGTACCGAGCTCGAATT
*Sma*I *Eco*RI

Fig. 1. Nucleotide sequences of $(LRE\text{-}3A)_4$ and $(LRE\text{-}3.6)_4$.

2. Materials and methods

2.1. Materials

Restriction endonucleases, bacteriophage T4 polynucleotide kinase and ligase, were obtained from USB and Sigma. Exonuclease III was from PROMEGA. Radiochemicals were from Amersham.

2.2. DNAs

Monomers of LRE-3A and LRE-3.6 were ligated with T4 ligase, separated on a 5% polyacrylamide gel and stained with ethidium bromide. Tetramers were electroeluted, filled with Klenow, and cloned in the *Sma*I site of pUC18. Recombinant plasmids were used to transform DH5α *E. Coli* cells. The DNA fragments were obtained by digesting the recombinant plasmids with *Eco*RI–*Hin*dIII. The inserts were purified on polyacrylamide gels.

5′-terminal labelling was performed according to a standard procedure. To label DNA fragments only at one end, plasmid DNA was first digested with one enzyme, then 5′ labelled and finally restricted with the appropriate secondary enzyme. The fragments were separated on 1.5% (w/v) agarose gel electrophoresis and the band of interest was recovered by electroelution.

2.3. Nucleosomes

Nucleosomes were obtained from chicken erithrocyte nuclei digested with micrococcal nuclease and purified through 5–20% sucrose gradient ultracentrifugation according to the method of Forte et al. [10].

2.4. Reconstitution procedure

Nucleosomes were reconstituted on the 299 bp DNA fragment according to the salt dilution protocol

described by Drew and Travers [1]. Reconstitution was monitored on 5% polyacrylamide gel electrophoresis in 0.5 × TBE buffer (0.045 M Tris-borate, 0.001 M EDTA, pH 8).

Mononucleosomes were purified by 1.0% agarose gel electrophoresis [11].

2.5. Exonuclease III

Reconstituted samples were made in 66 mM Tris-HCl (pH 8), 3 mM $MgCl_2$, 1 mM 2-mercaptoethanol, and equilibrated at 30°C. Exonuclease III (Exo III) was added at a final concentration of 10–100 $U ml^{-1}$, and reactions were stopped by adding an equal volume of 15 mM EDTA, 10% (w/v) sodium dodecylsulfate, and heating at 100°C for 2 min. Samples were extracted with phenol, precipitated with ethanol, resuspended in sequencing gel loading buffer, and run on a polyacrylamide–urea denaturing gel. Gels were dried, autoradiographed and analysed with an LKB laser densitometer.

2.6. Theoretical prediction of nucleosome positioning

Theoretical prediction of nucleosome positioning was obtained by evaluating the distortion energy required to transform the intrinsic DNA superstructure in the nucleosomal shape for recurrent 145 bp tracts along the 299 bp sequences. The energy values are relative to those characterizing a straight DNA tract [2,3].

3. Results

3.1. Gel electrophoretic mobility of differently positioned histone octamers on $(LRE\text{-}3A)_4$ and $(LRE\text{-}3.6)_4$

Nucleosome assembly on $(LRE\text{-}3A)_4$ and $(LRE\text{-}3.6)_4$ was carried out in order to obtain only the mononucleosome complex. As it is possible to observe in Fig. 2, in all the experiments a substantial amount of free DNA was present. Under these conditions mononucleosome is the only complex present. This is confirmed by running reconstituted samples on a 1% agarose gel; only two bands are present, corresponding to naked DNA and to mononucleosome (data not shown). On the other hand, on a 5% polyacrylamide gel it is possible to observe different positions of the histone octamer along the DNA fragment, since they give rise to bands having different mobilities [4–6]. Histone octamer positions on DNA seem to determine nucleosome migration on a nucleoprotein polyacrylamide gel similarly to the way the position of a bend in a DNA fragment is linked to its retardation in polyacrylamide gel [6,12]. As previously shown, nucleosomes in which the

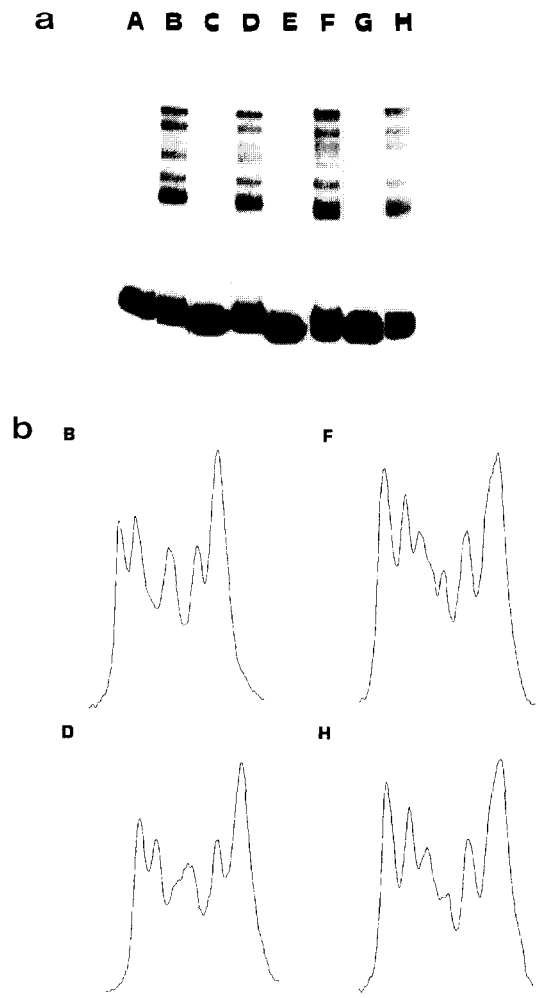

Fig. 2. (a) 5% polyacrylamide gel electrophoresis of $(LRE\text{-}3A)_4$ (lanes A–D) and $(LRE\text{-}3.6)_4$ (lanes E–H). Lanes A, C, E, G, free DNA; lanes B, D, F, H, nucleosomal complex. In lanes A, B, E, F, DNAs were 5′ labelled at the *Eco*RI site; in lanes C, D, G, H, at the *Hin*dIII site. (b) Densitometric profiles of the nucleosomal complexes autoradiographs shown in Fig. 2a.

histone octamer is located near the middle of the DNA fragment migrate as the slowest band, whereas end-positioned nucleosomes migrate in a faster band [6].

The main bands originating from nucleosome positioning on the two 299 bp long DNA fragments are six in number, with minor bands that could be identified as shoulders (Fig. 2).

Taking into account that the length of the two DNA fragments is about twice that of nucleosomal DNA, the number of nucleosome positions could be $(299 - 146)/10 = 15$; it is reasonable to predict $7 + 1$ differently migrating electrophoretic bands due to 7×2 nucleosome positions, equidistant from the DNA fragment ends, plus 1 central position. In Fig. 2 the most retarded band probably corresponds to nucleosome positions near the middle of the DNA fragments, while the other five bands should correspond to symmetric positions at the two sides, each differing by one B-DNA turn if the different nucleosomes have the same rotational phasing. The band with the highest mobility is the one most represented, suggesting a preference for the terminal nucleosome positions. The difference between the predicted and the experimentally detected number of nucleosome positions could reflect a partial separation of different bands on polyacrylamide gels.

3.2. Exo III nucleosome mapping on $(LRE\text{-}3A)_4$ and on $(LRE\text{-}3.6)_4$

The localization of nucleosome borders was obtained by Exo III digestion; the progress of this enzyme, which digests starting from the 3′-end, is impeded by the presence of a nucleosome. Prominent pauses in the time course of Exo III digestion should therefore signal the presence of major nucleosome positions.

Fig. 3a shows Exo III digests of naked DNA and reconstituted mononucleosome on $(LRE\text{-}3A)_4$ and $(LRE\text{-}3.6)_4$ 5′-end labelled on either strand. Since naked $(LRE\text{-}3A)_4$ and $(LRE\text{-}3.6)_4$ show some bands, probably due to sequence-specific pausing of the enzyme, care was taken to carry out Exo III digestion in the absence of free DNA. This was obtained by isolating mononucleosome from 1.0% agarose gel, where all the different bands detected in polyacrylamide gel collapsed in a unique large band [11].

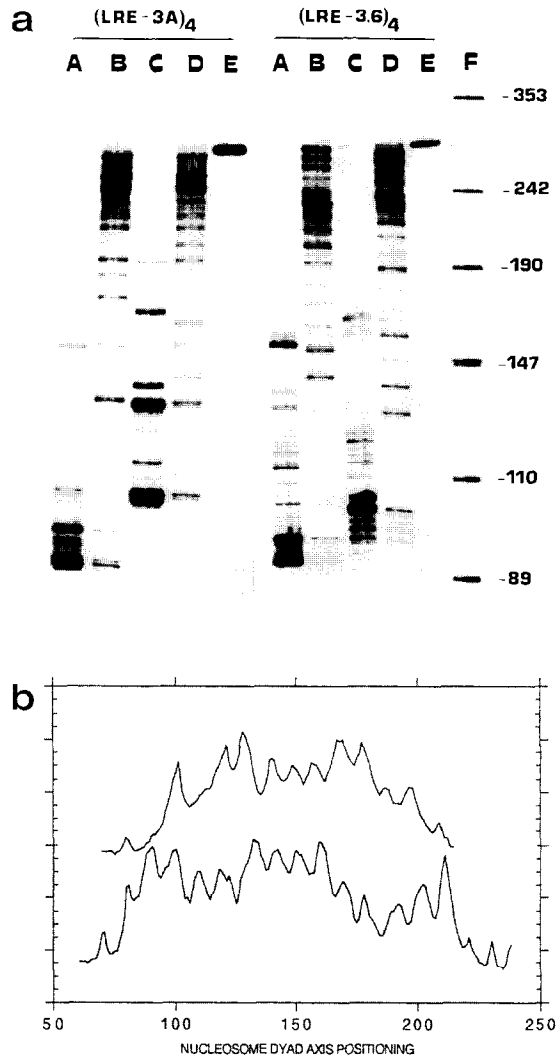

Fig. 3. (a) Autoradiograph of Exo III digestion patterns. The DNA was 5′-end labelled at the *Eco*RI (lanes A and B) or *HindIII* (lanes C and D) ends. Lanes A and C, free DNA; lanes B and D, reconstituted nucleosome; lane E, undigested DNA; lane F, molecular weight marker obtained by *Hpa*II digestion of pUC 18 DNA. (b) Nucleosome dyad axis positioning derived from Exo III stop patterns on either strand. $(LRE\text{-}3A)_4$, top; $(LRE\text{-}3.6)_4$, bottom.

The Exo III stops on naked DNA do not correspond to the stops found on the reconstituted complex.

Exo III digestion patterns appear as sets of regularly spaced bands, indicating that a number of differently populated sets of molecules with one well positioned nucleosome are present (Fig. 3a). To lo-

calize nucleosome stops with respect to the DNA sequence, the band patterns have been analysed as densitometric tracings in the range between 300 and 147 bp, which corresponds to a 'bona fide' nucleosome (146 bp). Nucleosome positions were assigned taking into consideration Exo III digestion from both directions. Exo III stops on the two DNA strands differing by 146 ± 2 bp identify the borders of the same nucleosome (see also ref. [11,13] for experimental details). The results are reported in Fig. 3b.

The main feature emerging from the distribution of nucleosome dyad axis translational positions is the presence of 12 main bands in the case of $(LRE\text{-}3A)_4$ (see Fig. 3b, top) and of 14 main bands in the case of $(LRE\text{-}3.6)_4$ (Fig. 3b, bottom) between 80 and 220 bp. In both cases, the phasing of the bands (as evaluated by Fourier transform) corresponds to 10 ± 0.3 bp; therefore, the bands can be attributed to different nucleosome translational positions with the same rotational phase.

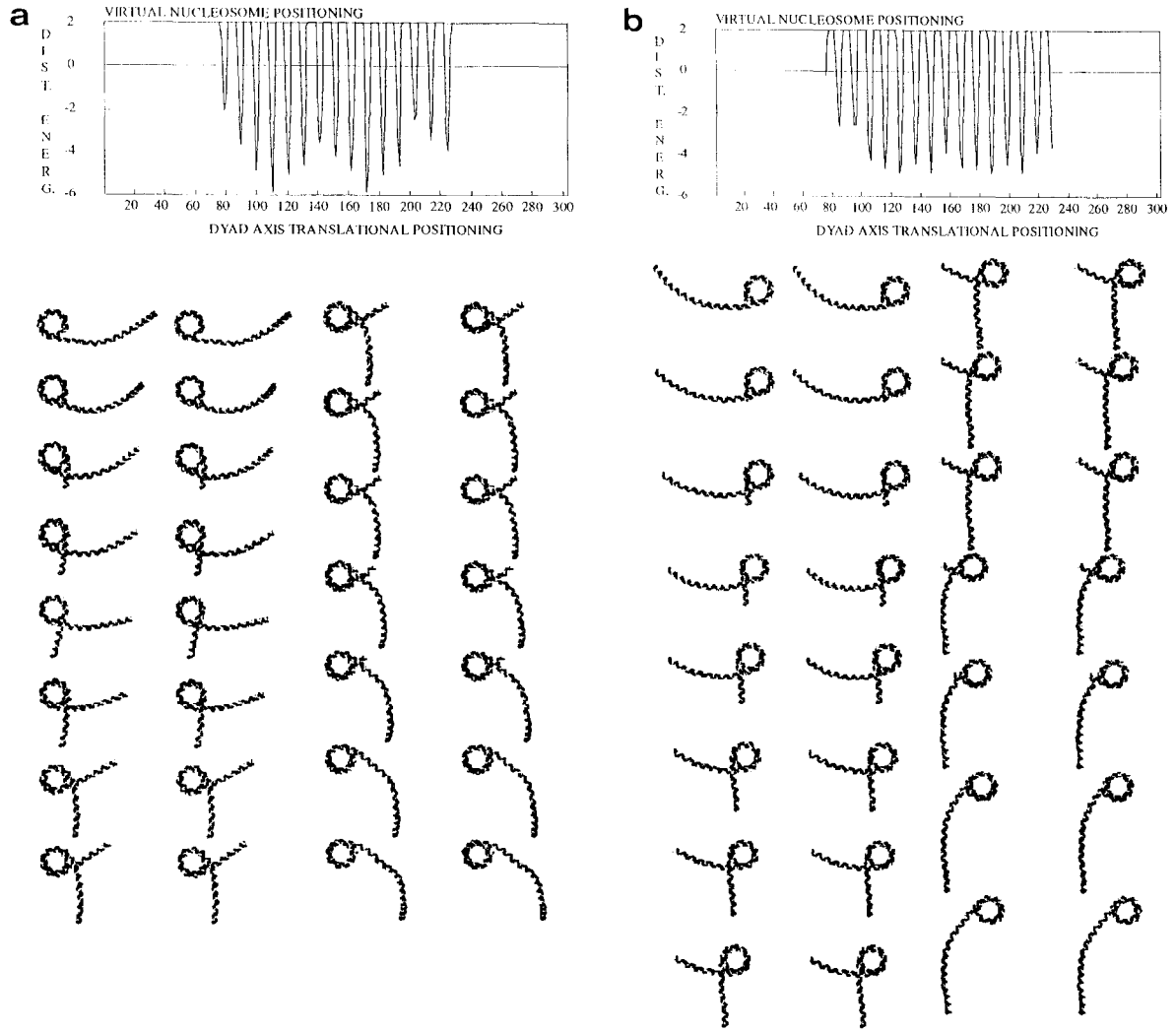

Fig. 4. Top: theoretical nucleosome positioning reported for each of the possible positions of the nucleosome dyad axis. The values of DNA distortion energy in forming nucleosome with respect to straight DNA are reported in kcal/mole of nucleosome. Bottom: stereoviews of nucleosome positions along the DNA fragment corresponding to each energy minimum. (a) $(LRE\text{-}3A)_4$; (b) $(LRE\text{-}3.6)_4$.

In analysing band distribution we have to consider two different parameters, namely the band position and the band height. It is worth observing that bands are symmetrically positioned with respect to the two terminals and thus should give rise respectively to 6 or 7 bands in the band shift assay, in agreement with the results reported in Fig. 2.

The band heights should represent the frequencies of nucleosome distributions, but, as previously reported [13], the heights could also be influenced by differences in Exo III digestion kinetics of the two strands, which are not completely eliminated by the averaging of the two distributions. Alternative explanations are the different chemical recognition between DNA and histones and/or entropic effects that favour peripheral positioning of nucleosomes. This last factor has been shown to cause changes of the binding constants associated with peripheral or middle site positioning of the CAP protein [14,15]. It is worth noting that the different heights of the bands corresponding to dyad positions differing by 62 bp inside the two LRE tetramers, corresponding to nucleosome positions spanning the same DNA sequence, demonstrate that Exo III kinetic effects are surely relevant.

3.3. Theoretical prediction of nucleosome positioning

To diminish the influence of errors intrinsic to all the experimental methods of nucleosome mapping, nucleosome positioning on the two DNAs has been calculated using a previously developed theoretical analysis [2,3]. Recurrent 145 bp tracts along a DNA sequence were constrained to deform in agreement with an 'open model' of the nucleosomal superstructure, characterized by two 60 bp tracts of a regular superhelix of 3/4 turns with 43 Å radius and 28 Å pitch interconnected by a straight tract 25 bp long. Such a model contains a dyad axis perpendicular to the superhelical axis, and was adopted on account of the superstructural features of nucleosomal DNA.

If $c(n)$ and $c'(n)$ are respectively the starting intrinsic curvature function of a 145 bp DNA tract and the final nucleosomal curvature function, the deformation potential energy E, adopting the first-order elasticity model, is given by:

$$E = \tfrac{1}{2} b \langle |c(n) - c'(n)|^2 \rangle$$

namely, a quantity proportional to the square of the modulus of the vectorial difference between the local curvatures, averaged over a 145 bp tract, where

$$c(n) = \sum_{n\text{th turn}} d(s) \exp(2\pi i s/\nu)$$

is the curvature at the position n of the sequence given in modulus and phase; b, the isotropic elastic bending constant of the 145 bp DNA tract:

$b = 1.45 \times 79$ kcal per mole of nucleosome, rad^{-2}

ν, the B-DNA periodicity; $d(s) = \rho - i\tau$, the local deviations of the sth dinucleotide step from the canonical B-DNA structure in terms of the roll, ρ, and tilt, τ, angles; and

$$c'(n) = -k \exp[2\pi i(n - 73)\alpha/145]$$

($k = 43{,}5°$ except for $60 \leq n \leq 85$ where $k = 0$); and α, the pitch angle of the nucleosomal superhelix = $\mathrm{tg}^{-1}\ 28/(2\pi \times 43)$. The deformation energy values are given with respect to that of a straight DNA tract.

Theoretical analysis results are reported in Fig. 4a for $(\text{LRE-3A})_4$, and in Fig. 4b for $(\text{LRE-3.6})_4$. At the top, the distortion energy minima are reported versus the nucleotide sequence. At the bottom, the stereoviews show 15 different nucleosome positions, referring to each energy minimum.

4. Discussion

A comparison between theoretical and experimental nucleosome mapping, derived from Exo III footprinting analysis, is reported in Fig. 5a in the case of $(\text{LRE-3A})_4$ and in Fig. 5b in the case of $(\text{LRE-3.6})_4$.

Two basic parameters characterizing nucleosome positioning (namely the number and the position of the nucleosome dyad axis along the nucleotide sequence) result in satisfactorily good agreement between theoretical and experimental analysis. The average dispersion of the dyad values is in the range ± 2 bp, and is thus significant in the comparison of theoretical and experimental methods.

The experimental evaluation of multiple nucleosome positioning by band shift assay on polyacrylamide gel relies on the influence of the form of the complex on its hydrodynamic properties (namely the

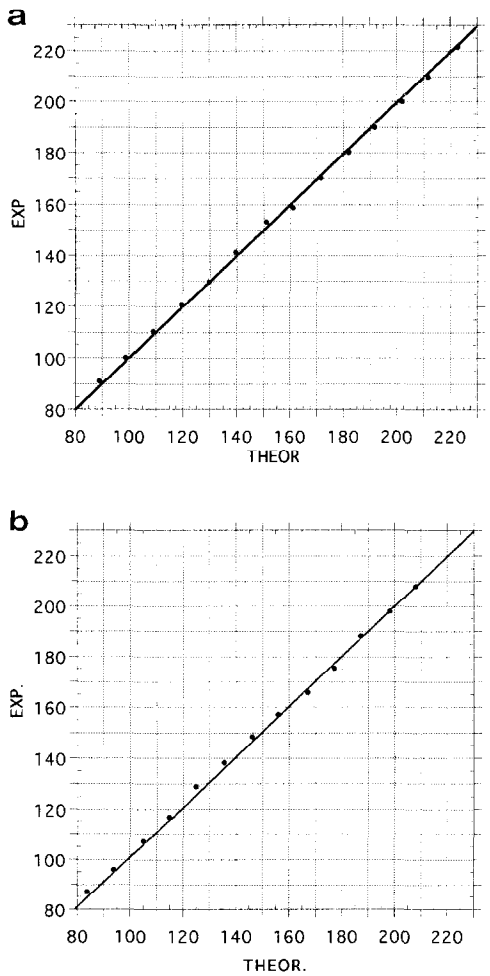

Fig. 5. Comparison between the nucleosome dyad axis positions deduced from ExoIII stops and the theoretical dyad positions. (a) $(LRE\text{-}3A)_4$; (b) $(LRE\text{-}3.6)_4$.

electrophoretic mobility). The possible different nucleosomes are represented by a reduced number of electrophoretic bands on account of the almost symmetric positioning of pairs of nucleosomes with respect to the ends of the DNA fragments, and to the resolving power of the 5% polyacrylamide gel. It is worth remembering that the six bands of the complex collapse into a unique large band on 1% agarose gel.

Considering the height of each band, indicating the frequencies of nucleosome distributions, noticeable differences are evident between theoretical and experimental nucleosome mapping. A general feature of theoretical nucleosome distribution is the regularity arising from the chemical and superstructural equivalence of 146 bp long nucleotide tracts, due to the multimerization. The experimental mapping appears irregular (see Fig. 3b) and suggests kinetic effects due to sequence-dependent Exo III digestion rate.

Nucleosome positioning could also be influenced by entropic effects arising from fluctuations of free DNA tracts of different lengths [14,15]. This could explain the different intensities of the electrophoretic bands reported in Fig. 2b. On the other hand, Exo III mapping does not show increased intensities of the terminal bands, probably on account of the simple averaging of the two strand cleavages.

In conclusion, experimental and theoretical nucleosome positioning result in fairly good agreement considering the number and the rotational phasing of nucleosome positions (Fig. 5). Chemical recognition between histones and DNA is not considered theoretically and is difficult to derive from nucleosome experimental mapping due to the inherent ambiguity of sequence-dependent Exo III kinetics of DNA cleavage, as is clearly demonstrated by the different frequencies of nucleosomes spanning the same sequences on the two tetramers examined.

Acknowledgements

Thanks are due to Dr A. Tufillaro for preliminary experiments and to R. Gargamelli for photographic help.

References

[1] H.R. Drew, A.A. Travers, J. Mol. Biol. 186 (1985) 773–790.
[2] D. Boffelli, P. De Santis, A. Palleschi, M. Savino, Biophys. Chem. 39 (1991) 179–188.
[3] P. De Santis, M. Fuà, A. Palleschi, M. Savino, Biophys. Chem. 46 (1993) 193–204.
[4] W. Linxweiler, W. Hörz, Cell 42 (1985) 281–290.
[5] S. Pennings, G. Meersseman, E.M. Bradbury, J. Mol. Biol. 220 (1991) 101–110.
[6] G. Meersseman, S. Pennings, E.M. Bradbury, EMBO J. 11 (1992) 2951–2959.
[7] R. Fluhr, P. Moses, G. Morelli, G. Coruzzi, N.-H. Chua, EMBO J. 5 (1986) 2063–2071.
[8] S. Cacchione, M. Savino, A. Tufillaro, FEBS Lett. 289 (1991) 244–248.

[9] F. Bordin, S. Cacchione, M. Savino, A. Tufillaro, Biophys. Chem. 44 (1992) 99–112.
[10] P. Forte, L. Leoni, B. Sampaolese, M. Savino, Nucleic Acids Res. 17 (1989) 8683–8694.
[11] P. De Santis, B. Kropp, L. Leoni, B. Sampaolese, M. Savino, Biophys. Chem. 62 (1996) 47–61.
[12] H.-M. Wu, D.M. Crothers, Nature 308 (1984) 509–513.
[13] S. Cacchione, M. Cerone, P. De Santis, M. Savino, Biophys. Chem. 53 (1995) 267–281.
[14] P. De Santis, M. Fuà, M. Savino, C. Anselmi, G. Bocchinfuso, J. Chem. Phys. 100 (1996) 9968–9976.
[15] D. Kotlarz, A. Fritsch, H. Buc, EMBO J. 5 (1986) 799–810.